Dielectronic recombination in He-like, Li-like, and Be-like highly charged ions in the *KLL* and *KLM* manifolds

A. P. Kavanagh,[1] H. Watanabe,[2] Y. M. Li,[3] B. E. O'Rourke,[1] H. Tobiyama,[2] N. Nakamura,[2] S. McMahon,[1] C. Yamada,[2] S. Ohtani,[2] and F. J. Currell[1]

[1]*Centre for Plasma Physics, International Research Centre for Experimental Physics, Queens University, Belfast, BT7 1NN, UK*

[2]*Institute for Laser Science and Department of Applied Physics and Chemistry, University of Electro-Communications, Chofu, Tokyo 182-8585, Japan*

[3]*Institute of Applied Physics and Computational Mathematics, Post Office Box 8009, Beijing 100088, People's Republic of China*

(Received 7 May 2008; revised manuscript received 15 October 2008; published 17 February 2010)

This paper reports a systematic study of the dependence on atomic number of the dielectronic recombination resonance strengths for He-like, Li-like and Be-like ions. Recent measurements of dielectronic recombination resonance strengths for the *KLL* and *KLM* manifolds for iron, yttrium, iodine, holmium, and bismuth are also described. The resonance strengths were normalized to calculated electron impact ionization cross sections. The measured resonance strengths generally agree well with theoretical calculations using the distorted wave approximation. However, *KLM* resonance strength measurements on high atomic number open-shell ions gave higher values than those suggested by calculations. Using recently measured data, along with existing results, scaling laws have been generated as a function of atomic number for He-like, Li-like, and Be-like ions in the *KLL* and *KLM* manifolds.

DOI: 10.1103/PhysRevA.81.022712 PACS number(s): 34.10.+x

I. INTRODUCTION

Obtaining accurate measured cross sections for charge-changing processes is challenging for highly charged ions (HCIs). Often in order to provide cross sections for atomic processes involving HCIs, scaling laws as a function of atomic number (Z) are generated. An example of such a scaling law is the He-like dielectronic recombination (DR) resonance strength scaling law developed by Watanabe *et al.* [1]. This paper reports a study of resonance strengths, involving a change in the principal quantum number of the target ion ($\Delta n \neq 0$), for open L-shell ions (Li- and Be-like) as a function of atomic number. Additionally new DR resonance strength measurements are presented for He-like ions. The scaling law of Watanabe *et al.* [2] has been updated using the new He-like measurements. Similar scaling laws for Li- and Be-like ions have also been generated for the first time, showing such scaling laws to be applicable to both open- and closed-shell systems.

The DR process is a two-stage resonant recombination process. It can have a very large rate coefficient and often is the dominant recombination mechanism in plasmas [3]. The first stage of DR, called dielectronic capture, is the capture of a continuum electron into an excited state of the target ion. The energy balance of the reaction is maintained by the excitation of an initially bound electron, of the target ion. If the doubly excited state radiatively stabilizes then the DR process is complete. As DR is a resonant process it can only occur when the target ions interact with electrons that have specific kinetic energies. DR is particularly interesting for HCIs due to the high electric fields the captured electron experiences. The high fields result in configuration mixing and correlation effects which must be accounted for by any theoretical modeling of the system. In HCIs of high-Z elements, quantum electrodynamic (QED) effects, which are normally considered minor corrections, grow to become major effects that can result in a measured resonance strength equal to twice the value predicted by models in which QED effects are ignored [4,5]. The required inclusion of correlation, configuration mixing, and QED makes atomic processes involving HCIs challenging to theoretically model.

The various types of DR processes are often split into two groups. The first involves the capture of high-energy electrons, with an associated change in the principal quantum number (n) of one of the core electrons in the ion ($\Delta n \neq 0$ transitions). The second involves the capture of low-energy electrons with no change in principal quantum number ($\Delta n = 0$ transitions). The $\Delta n \neq 0$ group is difficult to study experimentally due to the difficulty in measurement associated with high-energy electrons.

For $\Delta n \neq 0$ DR, in a given ion, the energies at which DR occurs are grouped into distinct manifolds. The manifolds are represented by a three-letter combination corresponding to an inverse Auger notation. Two letters of this combination correspond to the orbital shells in which the bound electron, that is, excited during DR, starts and finishes. The final letter corresponds to the shell into which the incident electron is captured. For example, *KLM* is either electron capture into the M shell with the bound electron being excited from the K to L shell or capture into the L shell with the bound electron being excited from the K to M shell.

There are various ways to measure the resonance strength of a resonance manifold, for example by measuring the resultant charge states after either colliding ions with electron targets in storage rings (see, for example, [6–8]), or by using crossed beams of ions and electrons [9]. In this paper an electron beam ion trap (EBIT) [10] was used to obtain the strength of the resonance manifold. An EBIT is an ion trap that uses an electron beam to create and trap highly charged ions. It is possible to measure photons emitted from the trapped ions as the electron beam is varied to deduce DR resonance strengths. The energy region of interest can be scanned by using either a

slow [11] or a rapid scan [12,13] of the energy of the electron beam. As an alternative to using photons, DR resonance strengths can also be measured by using ions extracted from an EBIT. One method is to measure the number of ions in a specific charge state while varying the length of time at a particular energy [14]. The DR resonance strengths can then be calculated from the rate of change of the number of ions in the charge state studied. Alternatively, the number of ions in each charge state can be monitored as the EBIT's electron beam energy is slowly changed [15]. It is a variation on the latter extracted ion method that will now be described.

II. METHOD

The measurements of DR resonance strengths were undertaken at the Tokyo electron beam ion trap (EBIT) [16,17]. The EBIT electron beam was set to a particular energy and sufficient time was given to reach charge state equilibrium in the ion trap. Ions will evaporate continuously from the trap. Those ions that escape out of the trap and pass through the electron beam collector electrode were passed along a beam line. The ion beam was passed through a charge separating magnet and ions with charge-to-mass ratios within a certain range impacted onto a microchannel plate (MCP). The resultant charge pulses at the back of the MCP were then detected on a resistive anode. The ions of interest can have a similar charge-to-mass ratio as ions created from background impurities. For example, He-like iron has almost the same charge-to-mass ratio as H-like nitrogen. In all cases in which the MCP produced overlapping charge pulses the pulse height of the individual MCP pulses was used to distinguish the ions under study. The energy of the electron beam in the EBIT was varied, in steps of several electron volts. For all measurements these steps were much smaller than the energy spread of the electron beam. The subsequent data analysis requires charge state equilibrium to be maintained and hence data acquired within 100 ms of a change in beam energy were not included. The experimental method is similar to that described by Watanabe *et al.* [2].

When the EBIT is in charge state equilibrium at any particular energy the following relationship can be written:

$$\frac{n_{q-1}}{n_q} = \frac{1}{\sigma_{q-1}^{EII}}\left[\left(\sigma_q^{DR}+\sigma_q^{RR}\right) + \frac{e}{j}\sum_{i=q}^{q_{\max}}\frac{n_i}{n_q}\left(n_0\sigma_i^{CX(i-q+1)}\bar{v}_i+\epsilon_i\right)\right], \quad (1)$$

where n_i is the number of ions in charge state i, n_0 is the number density of neutrals, $\bar{v}_i$ is the mean velocity of the ions, and j is the electron beam current density. The cross sections of radiative recombination, electron impact ionization, and dielectronic recombination are σ^{RR}, σ^{EII}, and σ^{DR}, respectively. It is important to note that $\sigma^{CX(i)}$ is the total cross section for more than $i-1$ electron capture from neutrals. ϵ_i is the ion escape rate, and $q_{\max}$ is the maximum charge state in the trap. The derivation of this equation is given in the supporting information. The ratio is composed of a slowly varying background due to slowly varying processes such as electron impact ionization and rapidly varying features due to resonant processes, such as dielectronic recombination. This is demonstrated by Fig. 1, which shows clear resonant peaks on a nonresonant background. To reflect the resonant and nonresonant parts Eq. (1) can be rewritten as

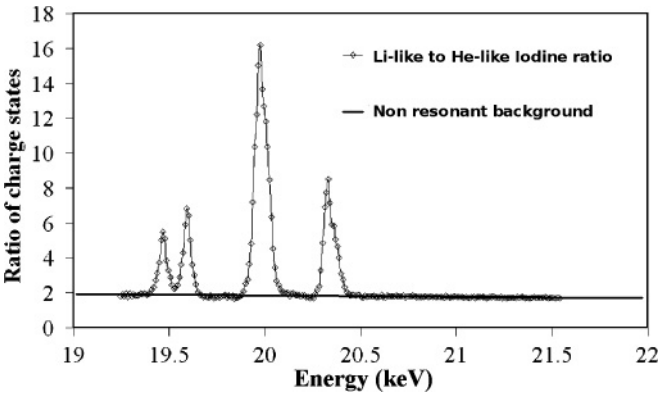

FIG. 1. Plot of the ratio of He-like iodine to Li-like iodine as a function of energy. The *KLL* resonant regions are clearly visible above the nonresonant background.

$$\frac{\sigma_q^{DR}}{\sigma_{q-1}^{EII}} = \frac{n_{q-1}}{n_q} - \sum_{i=0}^{q_{\max}-q}\alpha_i\frac{n_{q+i}}{n_q}, \quad (2)$$

where $\alpha_0 = \sigma_q^{RR}/\sigma_{q-1}^{EII} + (e/j)(n_0\sigma_q^{CX1}\bar{v}_q+\epsilon_q)/\sigma_{q-1}^{EII}$ and, for $i \geqslant 1$, $\alpha_i = (e/j)(n_0\sigma_{q+i}^{CX(i+1)}\bar{v}_{q+i}+\epsilon_{q+i})/\sigma_{q-1}^{EII}$ [2]. The terms α_i vary slowly with energy, but they are multiplied by a ratio of the number of ions in different charge states. The resultant terms $(\alpha_i\frac{n_{q+i}}{n_q})$ may then have a rapid variation with energy due to DR affecting the number of ions in either the q or the $q+1$ charge state. The dielectronic recombination manifolds for different ion charge states are at different energies. Hence the resonant features of $\alpha_i\frac{n_{q+i}}{n_q}$ may lie fully, or partly, within the nonresonant energy ranges of the measured ion ratio. The values of α_i depend on various charge exchange cross sections and escape rates, but these are not measured or evaluated in this method. Hence the shape of the resonant feature $\alpha_i\frac{n_{q+i}}{n_q}$ is not known.

The ion charge state ratio that the first alpha (α_0) is multiplied by $(\frac{n_{q-1}}{n_q})$ is the ratio of interest. As such its resonant features should not be removed. However, its nonresonant, slowly varying contribution can be removed by simply fitting to the nonresonant background of the measured ion ration and subtracting. The other alpha values can be estimated by using the maximum likelihood estimator (MLE) as described in [2]. The summation terms in Eq. (2) can then be evaluated and subtracted from the measured ratio, reducing Eq. (2) to

$$\frac{\sigma_q^{DR}}{\sigma_{q-1}^{EII}} = \left(\frac{n_{q-1}}{n_q}\right)^*, \quad (3)$$

where the starred ratio is the ratio after subtraction of the summation terms in Eq. (2). The effect of the summation terms is to increase the final value of the resonance strength

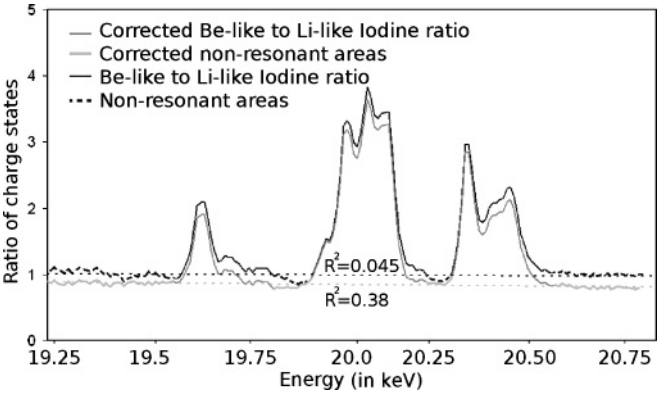

FIG. 2. Diagram showing the change in resonant features before and after the alpha terms have been corrected. Also shown is a linear fit with its R^2 value. The improved fitting in the nonresonant regions shows that some resonant features have been corrected.

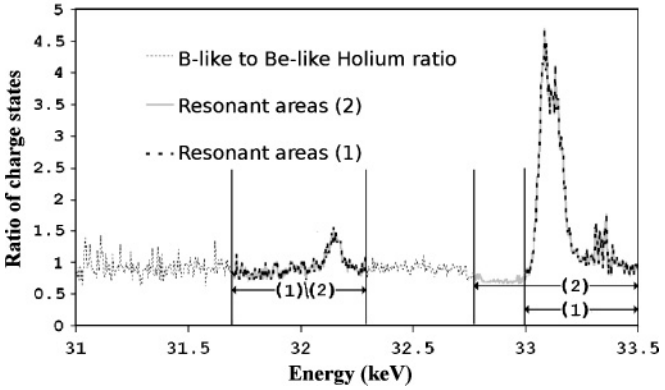

FIG. 3. A plot showing the B-like to Be-like holmium ratio in the energy range corresponding to the first two peaks in the *KLL* resonance manifold. Also shown is the area assigned as resonant (and therefore excluded from fitting) when the alpha values were calculated (1) and the new range (2) chosen to check if the alpha values varied. In this case the alpha terms did not vary.

calculated, giving at maximum a 5% systematic contribution in resonance strengths.

Rather than use the MLE method it is possible to to explore the parameter space, covered by $\{\alpha_i\}$ for $i > 0$, to find values which lead to the most successful removal of the effects of the terms $\alpha_i \frac{n_{q+i}}{n_q}$, for $i > 0$. The success can be quantified by evaluating the terms $\alpha_i \frac{n_{q+i}}{n_q}$, subtracting these from the measured ion charge state ratio ($\frac{n_{q+1}}{n_q}$), and measuring the goodness of fit of a slowly varying function (representing $\alpha_0 \frac{n_{q-1}}{n_q}$) to the nonresonant areas of the altered ratio. This method works since subtraction of the evaluated terms causes the resonant contribution of each term to be removed. Certain alpha values will provide the most complete removal of resonant features. The point in parameter space providing the most complete removal of resonant features will correspond to the fit with maximum value for the coefficient of determination [18] (see Fig. 2). The values at which this maximum occurs are taken to provide the α_i values for the correction given in Eq. (2). The variation of the value of the coefficient of determination when α_i is varied in the region of this maximum provides the uncertainty in α_i, a quantity which is used in evaluating the final resonance strength uncertainties. The goodness of fit can be measured by both the coefficient of determination and chi-squared and both methods give similar answers.

The number of alpha terms required is equal to $n - 1$, where n is the number of electrons in the target ion. For simple searching methods, the length of time required to complete this method scales with the power of the number of alphas required. It is this scaling that limits the use of this method to Li-like or Be-like ions. He-like systems only require one term to be corrected, namely $\alpha_0 \frac{n_{q-1}}{n_q}$. As this is removed by simple nonresonant background subtraction, for He-like systems, both the MLE and new methods are equivalent. An example of a resonant feature before and after alpha correction is shown in Fig. 2.

Interference between radiative and dielectric recombination occurs since the initial and final states in both recombination schemes are identical [19]. In the case of very highly charged ions, the profile of the interference might extend into the nonresonant region used in evaluating the $\alpha_i \frac{n_{q+i}}{n_q}$ terms, causing miscalculation. Even without interference, incorrect assessment of the start and end points of nonresonant regions can also cause miscalculation. In this case the miscalculation arises due to attempting to correct part of the studied resonant peak, as if it was a feature due to the $\alpha_i \frac{n_{q+i}}{n_q}$ terms. To guard against this, the $\alpha_i \frac{n_{q+i}}{n_q}$ terms were calculated several times, with differing end points chosen for the nonresonant regions. As the end points approach the resonant features at some point the alpha values start to systematically change. The end points that gave the largest nonresonant energy range before the resultant alpha values started to systematically change were used in the final calculation. It is not sufficient to start by selecting an energy range far from the resonant peaks because the resonant features of the terms being evaluated must be detectable. A demonstration of a test of alpha values with two different energy ranges is shown in Fig. 3.

Once the $\alpha_i \frac{n_{q+i}}{n_q}$ terms have been subtracted from the measured ion ratio, the starred ratio of Eq. (3) has been obtained. Equation (3) shows that, by rescaling the starred ratio, using electron impact ionization cross sections, the DR cross sections can be obtained. Hence calculated electron impact ionization cross sections were used to rescale the DR cross sections. The electron impact ionization cross sections were calculated using distorted wave calculations [20], with the ionic structure and energy levels obtained using the GRASP2 code [21,22]. Electron impact ionization cross sections were calculated at several points in the range of energies required. There is little variation in the electron impact ionization cross section across the measured energy range. Therefore, interpolation can be used to calculate intermediate energies. By rescaling and plotting one obtains the DR cross section plot convolved with the energy potential profile of the EBIT's electron beam.

The energy profile of the electron beam is of the order of tens of volts and varies depending on the electron beam current [23]. As the energy profile of the electron beam is much larger than the spacing between the individual DR transition

energies it is the resonance strength of the DR manifolds that is measured rather than individual cross sections. The resonance strength of a manifold is given by the equation

$$S = \int \sigma_q^{DR} dE, \tag{4}$$

where the integration limits are chosen to fully encompass all the peaks belonging to the manifold under consideration. In this analysis the limits of integration were set to include all effective cross section values greater than 10^{-25} cm^2. This approximation provides a negligible source of error, as was verified by checking convergence of the values produced when this threshold was changed. By using Eq. (3) the manifold's resonance strength is then given by

$$S = \sum \left(\frac{n_{q-1}}{n_q}\right)^* \sigma_{q-1}^{EII} \Delta E, \tag{5}$$

with the limits of the summation being equal to the integral limits of Eq. (4). Here ΔE is the energy per channel in the measured data.

The results obtained by this process were compared with theoretically calculated resonance strengths. Again the GRASP2 code was used to provide the initial energy levels, final energy levels, and the ionic structure. The dielectronic recombination cross sections were then obtained using the distorted wave approximation and included, when necessary, the effect of the generalized Breit interaction (GBI). The theoretical method used to calculate the DR cross sections is similar to that used in [24]. To compare the calculated cross sections to experimental results, the calculated cross sections were binned in energies with a bin width equal to the step in energy used during measurements. Then the binned cross sections were convolved with a Gaussian of FWHM similar to the profile of the electron beam. This procedure produces a convolved cross section plot that could then be compared to that experimentally obtained. The energy of the electron beam and thus of the electron ion interaction is difficult to determine accurately experimentally. Hence the absolute experimental energy is determined by shifting the experimental energy axis so the DR manifold peaks align with those theoretically calculated. An example of aligned effective cross section plots is shown in Fig. 4. By integrating the cross sections under the calculated resonant peaks the resonance strengths could be obtained. The experimental energy axis shifting is of the order of tens of electron volts and so makes no practical difference to the electron impact ionization cross section used for rescaling or thus the resonance strength measured.

The measurements obtained had several sources of uncertainty. These include statistical uncertainty, background fitting uncertainty, and uncertainty associated with the alpha value calculations. All these uncertainty sources were taken into account when calculating the error bars.

III. RESULTS

The experimental and calculated resonance strengths for He-like, Li-like, and Be-like ions of iron, iodine, holmium, and bismuth in the *KLL* and *KLM* resonances are given in Table I. Only *KLL* resonances were measured for yttrium.

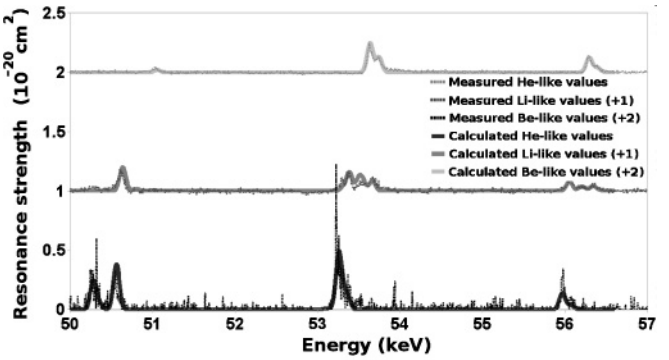

FIG. 4. Effective DR cross sections for He-like, Li-like, and Be-like bismuth ions in the *KLL* resonance region obtained both experimentally and theoretically (see main text for details). The theoretical cross sections have been binned and convolved with a Gaussian with a FWHM of 70 eV. For clarity, the Li-like and Be-like plots are offset by an amount indicated in the figure legend.

Previously, an empirical scaling law for He-like resonance strengths was determined by weighted least squares fitting of

$$S = \frac{1}{m_1 Z^2 + m_2 Z^{-2}}, \tag{6}$$

where Z is the atomic number and m_1 and m_2 are the free fit parameters [1]. By taking the present data and incorporating the results used in [1] the parameters m_1 and m_2 can be recalculated, to update the scaling law. The scaling formula is derived from the scaling predicted for an isolated H-like resonance. It does not include the effects of QED; however, the formula has been shown phenomenologically to be applicable to collective groups of resonances in He-like target ions [1]. This applicability is because in the low-Z and high-Z limits the asymptotic form of the sum of resonance strengths for a group of independent resonances is the same as the asymptotic form of Eq. (6). This applies to open- or closed-shell systems and hence this equation should be applicable to all the systems (He-, Li-, and Be-like) under study here.

For the He-like system, Eq. (6) was refitted, including the new data points, by weighted least squares with the weights obtained from the error bars in the included measurement. Figure 5 shows plots of the scaling law for He-like systems in the *KLL* and *KLM* manifolds. Equation (6) was then fitted to the other measured systems (Li- and Be-like). Figures 6 and 7 show scaling graphs for Li-like and Be-like ions in the *KLL* and *KLM* manifolds, respectively. For both *KLL* manifolds, in the region $Z < 30$, the fit is much better than the *KLM* fit, due to a previous highly accurate *KLL* measurement with neon ions [27]. In order to demonstrate the fitting uncertainty the error envelopes are also plotted for all three figures. The error envelope is obtained by varying the fitted parameters within 1σ of the best fit to obtain functions giving the maximum and minimal values. All the fitted parameters for the isoelectronic scaling functions plotted are given in Table II.

IV. DISCUSSION

The He-like scaling law has many data points for $20 < Z < 50$ and thus very good fitting for data points for $Z < 50$.

TABLE I. Table of the experimental and calculated resonances strength for He-like, Li-like, and Be-like ions of iron, yttrium, iodine, holmium, and bismuth in the *KLL* and *KLM* resonance regions. Resonance strengths are given in units of 1×10^{-20} cm^2 eV and the bracketed figures indicate the 1σ uncertainty level.

Element	Fe	Y	I	Ho	Bi
KLL					
He-like	64.1(11.5)	54.8(13.7)	36.2(2.2)	30.0(8.1)	19.9(4.4)
Calculated	76.6	55.0	36.2	26.7	22.4
Li-like	72.7(16.7)	34.4(8.3)	25.1(1.8)	19.1(4.6)	12.0(1.0)
Calculated	58.2	39.7	24.0	16.3	12.5
Be-like	50.9(17.8)	39.6(7.1)	20.3(2.0)	17.9(4.8)	7.99(0.4)
Calculated	51.8	35.0	21.9	13.5	8.36
KLM					
He-like	48.1(8.7)	–	19.7(2.2)	11.5(1.4)	9.06(2.36)
Calculated	43.0	23.8	13.9	9.62	7.72
Li-like	24.2(5.6)	–	16.8(1.7)	10.1(1.3)	9.09(1.64)
Calculated	27.4	14.3	8.38	7.52	5.81
Be-like	35.7(12.5)	–	15.1(1.5)	9.00(1.17)	6.14(0.92)
Calculated	33.1	17.4	10.8	6.44	5.22

For the He-like resonance strength measurements for higher atomic numbers, in the *KLL* manifold, the scaling law starts to predict smaller values than those measured. This deviation could be due to the emergence of QED effects which are not included in the scaling model. For example, GBI is known to alter the strength of cross sections for high-atomic-number ions [28]. However, more measurements would be required to properly test this.

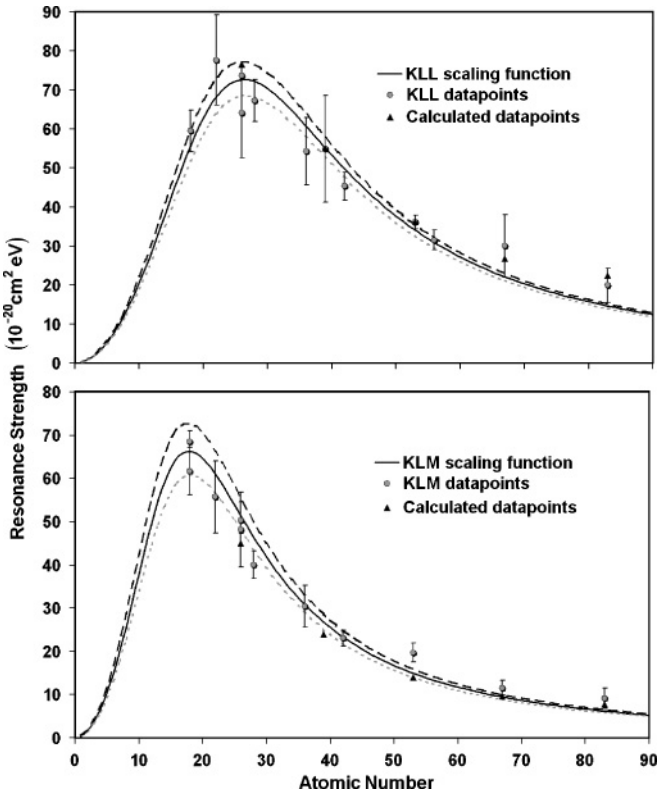

FIG. 5. Plots of He-like ion resonance strengths in the *KLL* and *KLM* manifolds against atomic number. Calculated values obtained using the distorted wave method are also plotted. A fitted scaling function based on Eq. (6) is also plotted. The scaling law was obtained by fitting to the existing [14,25,26] and new data points. The dotted and dashed lines indicate the 1σ error envelope as described in the main text.

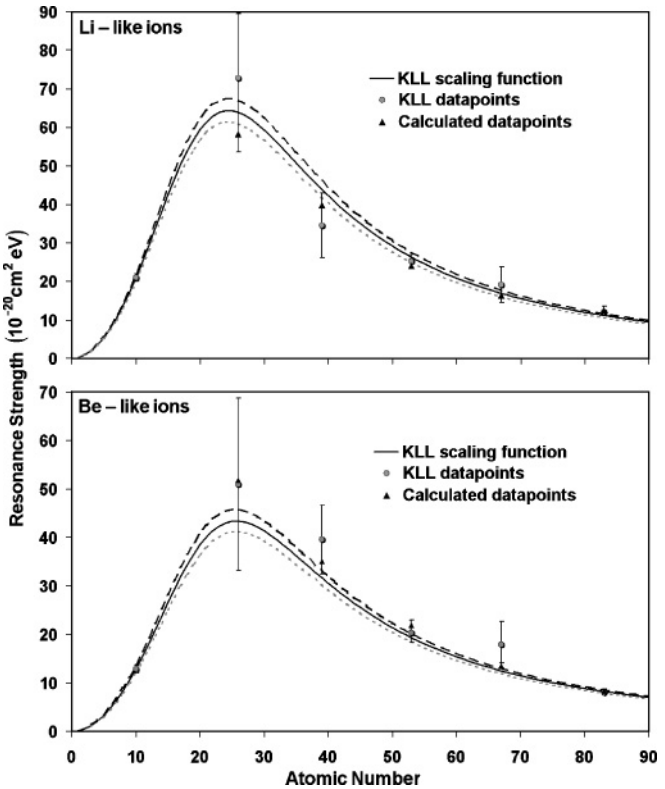

FIG. 6. Plot of Li-like and Be-like ion resonance strengths in the *KLL* manifold against atomic number. Calculated values obtained using the distorted wave method are also plotted. Both species of ions have the fitted scaling function plotted. The neon results were obtained from [27]. The dotted and dashed lines indicate the 1σ error envelope as described in the main text.

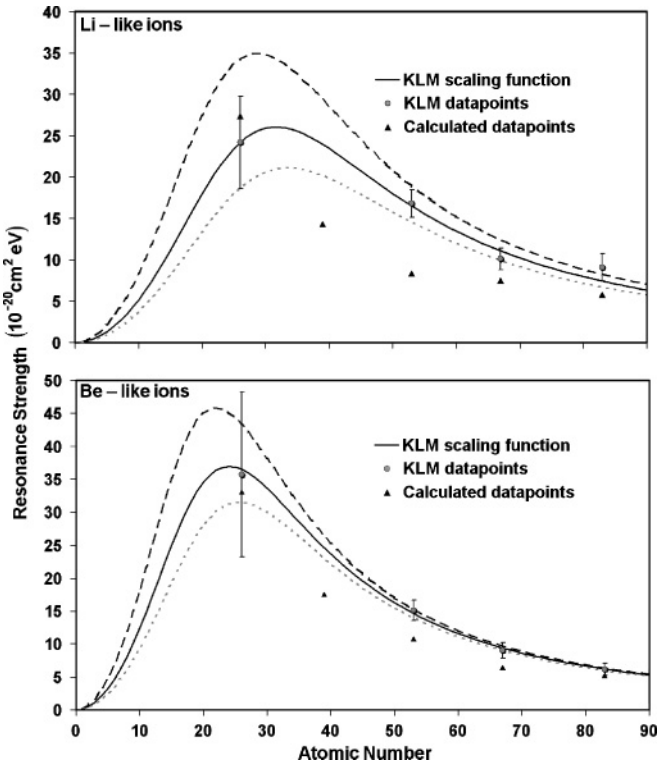

FIG. 7. Plot of Li-like and Be-like ion resonance strengths in the *KLM* manifold against atomic number. Calculated values obtained using the distorted wave method are also plotted. Both species of ions have the fitted scaling function plotted. The dotted and dashed lines indicate the 1σ error envelope as described in the main text.

In contrast to the He-like system, there are fewer measurements available for the Li- and Be-like *KLL* resonance manifolds. The fits in these systems are highly constrained by the bismuth data point so it is not possible to make any meaningful assertion about the breakdown of Eq. (6) in these cases. It is however clear that the fit to Eq. (6) has useful predictive power for the *KLL* resonance strength of elements for which data are not available.

For the open-shelled *KLM* systems, the large error envelope in the predicted resonance strength, especially for ions with $Z < 30$, makes producing firm conclusions difficult. The large uncertainty arises from the lack of *KLM* DR resonance strength measurements of low-Z ions. Also, difficulty obtaining the iron measurement resulted in large error bars, and thus the weighted fitting is not very constrained in the low-Z range. In the future, several low-Z measurements would significantly help in reducing the uncertainty and greatly extend the applicability of the scaling formula.

TABLE II. Table of parameters obtained by fitting the function $\frac{1}{m_1 Z^2 + m_2 Z^{-2}}$ to various sets of measurements of dielectronic recombination varying isoelectronically. The data points used are given in [1] and in Table I. The bracketed figures indicate the 1σ uncertainty level.

Ion	Manifold	m_1 (cm^{-2} eV^{-1})	m_2(cm^{-2} eV^{-1})
He-like	*KLL*	$9.86(4) \times 10^{14}$	$4.80(38) \times 10^{20}$
He-like	*KLM*	$2.36(15) \times 10^{15}$	$2.42(29) \times 10^{20}$
Li-like	*KLL*	$1.30(7) \times 10^{15}$	$4.65(21) \times 10^{20}$
Li-like	*KLM*	$1.91(19) \times 10^{15}$	$1.92(74) \times 10^{21}$
Be-like	*KLL*	$1.75(8) \times 10^{15}$	$7.60(48) \times 10^{20}$
Be-like	*KLM*	$2.34(8) \times 10^{15}$	$7.8(26) \times 10^{20}$

All results were obtained via normalization to electron impact ionization cross sections supplied from distorted wave calculations. The distorted wave cross sections were compared to those obtained by using the Lotz scaling law [29], to give a rough check on their values. In all cases the distorted wave and Lotz values were as close as can be expected given the limitations of the Lotz formula.

All measured *KLL* and He-like *KLM* resonance strengths agree, within uncertainties, with calculated values. *KLM* resonance strengths of the open-shell Li-like and Be-like systems do appear to have a clear discrepancy between the measured and calculated values. The reason for the discrepancy is unknown at present and again points to the need for more measurements of this type. It is important to note that the correction in going from Eq. (2) to Eq. (3) (i.e., removal of the summation terms) only gives at most a 5% change in the resonance strength. Therefore this process cannot be the cause of the discrepancy.

ACKNOWLEDGMENTS

The authors wish to thank the Institute for Laser Science and Department of Applied Physics and Chemistry at the University of Electro-Communications for the use of its facilities. This work was funded by the British Council and the Natural Science Foundation of China under Grant No. 10674020. A. P. Kavanagh and F. J. Currell also thank the Royal Society, whose funding made their participation possible.

[1] H. Watanabe *et al.*, J. Phys. B **35**, 5095 (2002).
[2] H. Watanabe *et al.*, Phys. Rev. A **75**, 012702 (2007).
[3] K. R. Karim and C. P. Balla, Phys. Rev. A **37**, 2599 (1998).
[4] C. Brandau *et al.*, Phys. Rev. Lett. **91**, 073202 (2003).
[5] N. Nakamura *et al.*, J. Phys.: Conf. Ser. **88**, 012066 (2007).
[6] S. Schippers *et al.*, Astrophys. J **555**, 1027 (2001).
[7] A. Lampert *et al.*, Phys. Rev. A **53**, 1413 (1996).
[8] C. Brandau *et al.*, Radiat. Phys. Chem. **75**, 1763 (2006).
[9] D. S. Belic *et al.*, Phys. Rev. Lett. **50**, 339 (1983).
[10] M. A. Levine *et al.*, Phys. Scr. **T22**, 157 (1988).
[11] A. J. Gonzalez-Martinez, J. R. C. Lopez-Urrutia, and J. Ullrich, Radiat. Phys. Chem. **75**, 1771 (2006).
[12] H. Watanabe *et al.*, J. Phys. B **34**, 5095 (2001).
[13] M. B. Schneider *et al.*, Phys. Rev. A **45**, R1291 (1992).
[14] D. R. DeWitt *et al.*, Phys. Rev. A **47**, R1597 (1993).
[15] R. Ali, C. P. Bhalla, C. L. Cocke, and M. Stockli, Phys. Rev. Lett. **64**, 633 (1990).

[16] F. J. Currell *et al.*, J. Phys. Soc. Jpn. **65**, 3186 (1996).
[17] N. Nakamura *et al.*, Rev. Sci. Instrum. **69**, 694 (1998).
[18] J. P. Barrett, Am. Stat. **28**, 19 (1974).
[19] D. A. Knapp *et al.*, Phys. Rev. Lett. **74**, 54 (1995).
[20] D. L. Moores and K. J. Reed, J. Phys. B **28**, 4861 (1995).
[21] I. P. Grant *et al.*, Comput. Phys. Commun. **21**, 207 (1980).
[22] K. G. Dyall, Comput. Phys. Commun. **55**, 425 (1989).
[23] H. Kuramoto *et al.*, Phys. Scr. **T92**, 351 (2001).
[24] Y. M. LI. *et al.*, J. Plasma Fusion Res. **79**, 52 (2003).
[25] A. J. Smith *et al.*, Phys. Rev. A **62**, 052717 (2000).
[26] T. Fuchs *et al.*, Phys. Rev. A **58**, 4518 (1998).
[27] B. J. Wargelin, S. M. Kahn, and P. Beiersdorfer, Phys. Rev. A **63**, 022710 (2001).
[28] C. J. Fontes, D. H. Sampson, and H. L. Zhang, Phys. Rev. A **47**, 1009 (1993).
[29] W. Lotz, Z. Phys. **216**, 241 (1968).